Contents lists available at ScienceDirect

Biomaterials

journal homepage: www.elsevier.com/locate/biomaterials

Fabrication of self-assembling D-form peptide nanofiber scaffold d-EAK16 for rapid hemostasis

Zhongli Luo [a,*], Shunkang Wang [a], Shuguang Zhang [b,**]

[a] West China Hospital, Laboratory for Nanobiomedical Technology, Sichuan University, Chengdu, Sichuan 610065, China
[b] Center for Biomedical Engineering NE47-379, Massachusetts Institute of Technology, 77 Massachusetts Avenue, Cambridge, MA 02139-4307, USA

ARTICLE INFO

ABSTRACT

We previously reported a class of designer self-assembling peptides that form 3-dimensional nanofiber scaffolds using only L-amino acids. Here we report that using D-amino acids, the chiral self-assembling peptide d-EAK16 also forms 3-dimensional nanofiber scaffold that is indistinguishable from its counterpart l-EAK16. These chiral peptides containing all D-amino acids, d-EAK16, self-assemble into well-ordered nanofibers. However with alternating D- and L-amino acids, EA*K16 and E*AK*16, showed poor self-assembling properties. To fully understand individual molecular building blocks and their structures, assembly properties and dynamic behaviors for rapid hemostasis, we used circular dichroism, atomic force microscopy and scanning electron microscopy to study in detail the peptides. We also used rheological measurement to study the hydrogel gelation property. Furthermore, we used an erythrocyte-agglutination test and a rabbit liver wound healing model, particularly in the transverse rabbit liver experiments, to examine rapid hemostasis. We showed that 1% d-EAK16 for the liver wound hemostasis took ~20 s, but using 1% of E*A*K16 and EA*K16 that have alternating chiral D- and L-amino acids took ~70 and ~80 s, respectively. We here propose a plausible model not only to provide insights in understanding the chiral assembly properties for rapid hemostasis, but also to aid in further design of self-assembling D-form peptide scaffolds for clinical applications.

1. Introduction

Design of functional biological materials that specifically meet the needs of scientific, technological and medical challenges would transform clinical medicine and nanobiotechnology. We previously reported the discovery of a class of natural self-assembling peptides [1]. We subsequently not only expanded designer materials further using 20 natural L-amino acids, but also developed various applications in many areas including: 1) solubilizing and stabilizing membrane proteins that are known to be notoriously difficult for biochemical and structural studies [2–4], 2) controlling drug delivery of molecular medicine [5–8], 3) development of a solar energy nanobio energy harvesting device [9,10], 4) 3-D tissue cell cultures [11–15], 5) use in tissue engineering and regenerative medicine [16–20].

A number of designer self-assembling peptides using L-amino acids have been extensively studied [21–28]. We have recently

demonstrated that D-form self-assembling peptide d-EAK16 composed of only D-amino acids has a stable secondary structure tolerating temperature (90 °C), pH changes and ionic strength [29]. Furthermore, we have demonstrated the advantage of D-form peptides over L-form peptides particularly to the D-form nanofibers resistant to proteases digestion [30]. We here report our study of four chiral self-assembling peptides d-EAK16, l-EAK16, EA*K16 and E*AK*16 for rapid hemostasis in a rabbit liver wound healing model.

In order to better understand the individual molecular and material building blocks, their structures, assembly properties, dynamic behaviors and application for rapid hemostasis, we carried out systematic studies. We showed that the d-EAK16 peptide formed stable secondary structures. AFM images showed d-EAK16 self-assembled into ordered nanofibers and the formation of nanofibers in a time-dependent dynamic process. However, this was not true for D- and L- alternating amino acids in EA*K16 and E*AK*16. The rheological studies and agglutinating activity examination showed there were significant differences between all D-amino acid-peptide d-EAK16, and mixed D- L-amino acid-peptides EA*K16 and E*AK*16. In order to provide deeply insights into the mechanism of hemostasis of D-peptide scaffolds we also

* Corresponding author.
** Corresponding author.
E-mail addresses: Zhongliluo@163.com (Z. Luo), Shuguang@mit.edu (S. Zhang).

propose a plausible model to it, which aims to help further design a new class of nanomaterials for potential clinical applications.

2. Materials and methods

2.1. Peptides synthesis and purification

Peptide d-EAK16 sequence containing all D-amino acids is Ac-(Ala-Glu-Ala-Glu-Ala-Lys-Ala-Lys)$_2$-CONH$_2$, and l-EAK16 sequence containing all L-amino acids is Ac-(Ala-Glu-Ala-Glu-Ala-Lys-Ala-Lys)$_2$-CONH$_2$; EA*K16 sequence is Ac-(^{D}Ala-Glu-^{D}Ala-Glu-^{D}Ala-Lys-^{D}Ala-Lys)$_2$-CONH$_2$ and E*AK*16 sequence is Ac-(Ala-^{D}Glu-Ala-^{D}Glu-Ala-^{D}Lys-Ala-^{D}Lys)$_2$-CONH$_2$ (D: the D-amino acid). These peptides were commercially custom-synthesized by solid-phase peptide synthesis (Chengdu CP Biochem Co., Ltd, Chengdu, China). The peptides were acetylated and amidated at the N-terminus and C-terminus, respectively. Purified by HPLC and characterized by mass spectroscopy. The purity of the d-EAK16 was 98.11% and of the l-EAK16, 95.02%, EA*K16 was 95.73% and E*AK*16 of the 95.50%. The lyophilized white fluffy powder was stored at 4 °C. Stock solutions of the peptides were prepared at concentrations of 1.0, 10.0 and 20.0 mg/ml in water (Millipore Milli-Q system, U.S.A) and stored at 4 °C before use.

2.2. Circular dichroism spectroscopy

The samples consisted of 1.0 mg/ml peptide aqueous stock dissolved and adjusted to 100 μM in solution in water. A sample of 500 μl added in a CD cuvette with a 2 mm path-length. Measurements are carried out on an Aviv400 CD spectrometer (Aviv Biomedical, Lakewood, NJ, U.S.A). Incubated the samples at 37 °C with an increment of 2 °C, equilibration 30 s, measured from 190 to 260 nm, averaged over 3 s through the entire wavelength range, and took the 190–250 nm analysis.

2.3. Atomic force microscopy

The peptide solution was prepared 0.1–10 mg/ml, applied 5–10 μl peptide solution and deposited onto a freshly cleaved mica surface. To absorb the peptide on the surface, each aliquot was left for 30–60 s and then washed with 100 μl deionized water at least 3 times, then dried in air and imaged immediately. The images were obtained to scan the mica surface in air by AFM (Hitachi SPM400, Japan) running in Tapping Mode. Soft silicon cantilevers were chosen (SI-DF2000, K-A102001604, Japan) with spring constant of 1–5 N/m and tip radius of curvature of 5–10 nm. When imaging soft biopolymers with AFM at high resolution, it is important to minimize the tip tapping force. AFM images were taken at 512 × 512 pixels resolution and displayed topographic images of the samples, in which the brightness of features increases as a function of height. Typical scanning parameters were as followed. Scan Mode: 2ch Simul; Data type: Topography (Servo); Area/Speed 1000 × 1000 nm/1.0–1.5 Hz; Amp. Ref.: -0.1 to -0.3; Vib. Voltage: 1.0–2.0 V, Bias: 0.000 V; Integral and Proportional gains 0.03–0.3 and 0.1–0.5 respectively.

2.4. Scanning electron microscopy

Prepared 2–10 mg of the peptides powder and added to 200–1000 ml phosphate-buffered saline (PBS, pH = 7.2) to self-assembly overnight. Dry in vacuum tube and then covered with gold and used SEM (JSM-5900, JEOL, Japan) to examine the nano-structures. The specimens were examined from 5000–20,000× magnifications. For d-EAK16 see reference [30].

2.5. Rheometry assays

Rheology experiments were performed on a 20 mm parallel plate controlled rheometer (TA Rheology Advantage, AR2000EX, U.S.A). Samples were dissolved in water at a concentration of 20.0 mg/ml, sonicated for 10 min, and stored at 4 °C in a refrigerator for a night. The rabbit blood was added to some anticoagulant buffer solution and stored at 4 °C for a night before test. Combined the peptide solution to the rabbit blood quickly as a volume ratio 1:1 (peptide concentration is 10.0 mg/ml) and then loaded ~500 μl with analysis. Experiment option of value limit for flow torque is 10.00 μN.m and velocity is 0.001 rad/s, for oscillation torque is 5 μN.m and velocity is 0.00001 rad/s and raw phase is 170°. All step types are normal force from 0.1000 to 50.00 N. The peptides were allowed to gel ~30 s at room temperature as the testing was running continually to 10 min and then for another again.

2.6. Examination of agglutinating activity

The agglutinating activity of peptides at different concentrations was tested in a 96-plate. The peptide samples and the rabbit erythrocytes were combined at 1:1 volume, vibrated for 10 min and stored at 4 °C for 2 h and the samples were observed under an optical microscope.

2.7. Hemostasis of rabbit liver wound healing model

In the transverse rabbit liver wound healing experiments, 20 white New Zealand rabbits (1–3 kg, random distribution of male and female), chose 3 bigger liver in each rabbit and made a sagittal liver cut about 1.5 cm, 0.1–0.2 cm and 0.2–0.4 cm in length, width and depth. Applied 200 μl of 10 mg/ml (~1% (wt/vol)) peptide solution into the wound and recorded the hemostasis time. Every peptide solution was repeated 10 times on different rabbits and recorded an average time for hemostasis. Here we focus on the chiral peptides themselves as a catalyst to hemostasis and do not estimate the clinical relevance of our findings, so some positive controls (current treatment protocol, other hydrogels) are not in consideration here. In addition, we chose two rabbits as a negative control, namely without adding peptides, and found the hemostasis time were 80–120 s. The peptide powder was dissolved in water (Millipore, Milli-Q system, U.S.A.) at 10 mg/ml, vibrated for 10 min, and then stored them at 4 °C for 16 h before use. All the study followed the Animal ethics committee rule and approved by the Animal Ethics Committee of the Sichuan University.

2.8. Cell cultures

The SMMC7721 cell strain was originally purchased from American Type culture Collection (ATCC, Rockville, MD, USA). It was a gift from West China Hospital of Sichuan University for this study. The cells were grown in 10% fetal bovine serum (Invitrogen, Grand Island, USA).

2.9. Molecular modeling

Molecular models of these peptides were constructed using free modeling software from China (Hyperchem professional version 7.5, http://www.hyper.com; VMD1.8.7, http://www.ks.uiuc.edu/Research/vmd/). The software package was run on a PC computer.

3. Result and discussion

3.1. Molecular models of 2 chiral pairs of d-EAK16 and l-EAK16 or EA*K16 and E*AK*16

We here present 2 chiral pairs of molecular models of EAK16 (Fig. 1). These peptides have identical sequences but are composed of amino acids of different chiral form: all D-amino acids in d-EAK16 and all L-amino acids in l-EAK16 (Fig. 1A,B). However, in EA*K16 sequence only A* is D-alanine, the others are L-amino acids (Fig. 1C). In E*AK*16 only Ala is L-amino acid, E* and K* are D-amino acids (Fig. 1D). Although the pairs of d-EAK16 and l-EAK16 or EA*K16 and E*AK*16 structures appear to be similar, their properties and functions are quite dissimilar.

3.2. Secondary structural properties of the chiral d-EAK16, l-EAK16, EA*K16 and E*AK*16

We previously reported that l-EAK16 forms an exceedingly stable β-sheet structure [1]. The CD spectrum of d-EAK16 indeed has an inverted β-sheet with a maximum ellipticity at 218 nm and a minimum ellipticity at 193 nm at physiological temperature (Fig. 2A). The CD spectrum of d-EAK16 has a near perfect mirror image of l-EAK16 spectrum. Comparing to EA*K16, EA*K16 has a maximal ellipticity at 208 nm and a minimal ellipticity at 199 nm. Likewise, E*AK*16, which is an enantiomer of EA*K16, has a minimal ellipticity at 208 nm and a maximal ellipticity at 199 nm. They are almost symmetrical to each other in water (Fig. 2B). The secondary structures of EA*K16 and E*AK*16 are neither a typical β-sheet nor an α-helix formation and seem to be uncharacterized-they appear to be closer to "random coil" CD spectra. The mixed chiral amino acids in the peptides indeed drastically alter the secondary structures, especially for the D-amino acid substitutions that disrupt the β-sheet structure in either all L- or all D-form peptides.
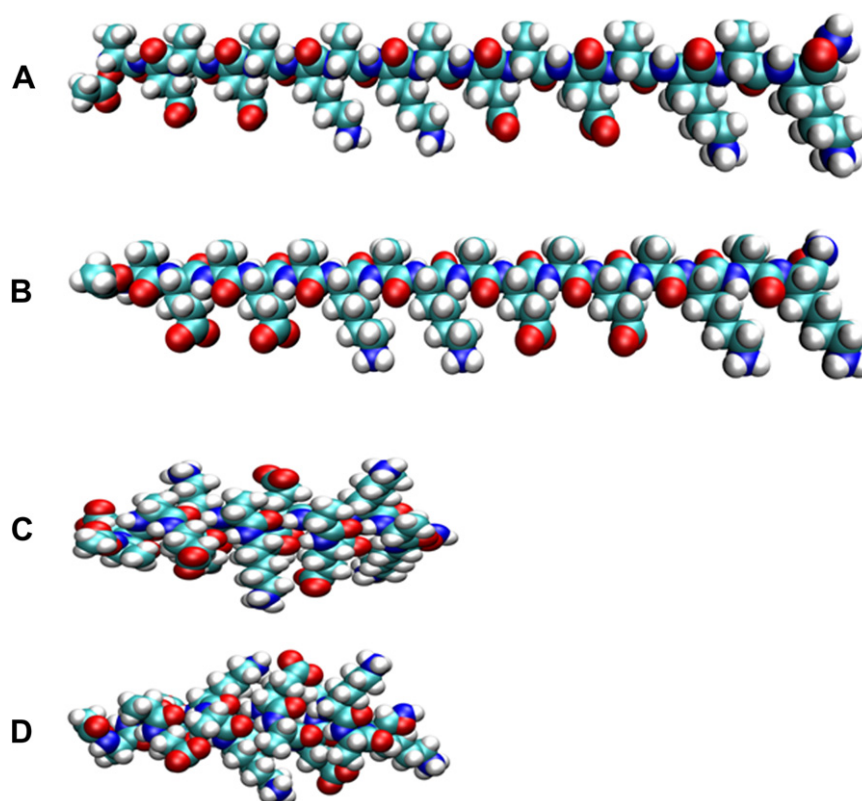
Fig. 1. Molecular models of 2 pairs of chiral peptides. A) d-EAK16; B) l-EAK16; C) EA*K16; D) E*AK*16. * refers to the ᴅ-form amino acids. All peptides are modeled in the extended (N–>C). Color code: hydrogen = white, carbon = cyan, oxygen = red and nitrogen = blue.

3.3. Factors that affect peptide self-assembly

3.3.1. The influence of concentration upon peptide self-assembly

The self-assembling peptide d-EAK16 nanofiber formation is affected by a certain concentration. In 100 μM solution, although nanofibers were visible, these nanofibers do not easily form a 3D scaffold. This is likely due to a low density of nanofibers (Fig. 3A). In contrast, in 1200 μM solution, the well-ordered nanofibers form a scaffold that was clearly visible (Fig. 3A). These results suggest a higher concentration of d-EAK16 in solution produces a higher density of nanofibers, thus forming a hydrogel. These highly hydrated nanofibers with numerous lysine and glutamic acid on the surface perhaps organize water molecules through numerous nanopores. Similar observations were made with other self-assembling peptides RADA16 [31]. This hydration phenomenon is similar to that found in the jellyfish which itself is highly hydrated containing >95% water. Therefore, in the subsequent hemostasis studies, we used 1% or higher concentration solutions to achieve the optimal hemostasis of rabbit liver wound healing models.

3.3.2. Dynamic self-assembling process as a function of time

We next asked what the time duration of the self-assembling process in NaCl solution would be, given it is known from previous studies that salts accelerate the self-assembly process, whereas
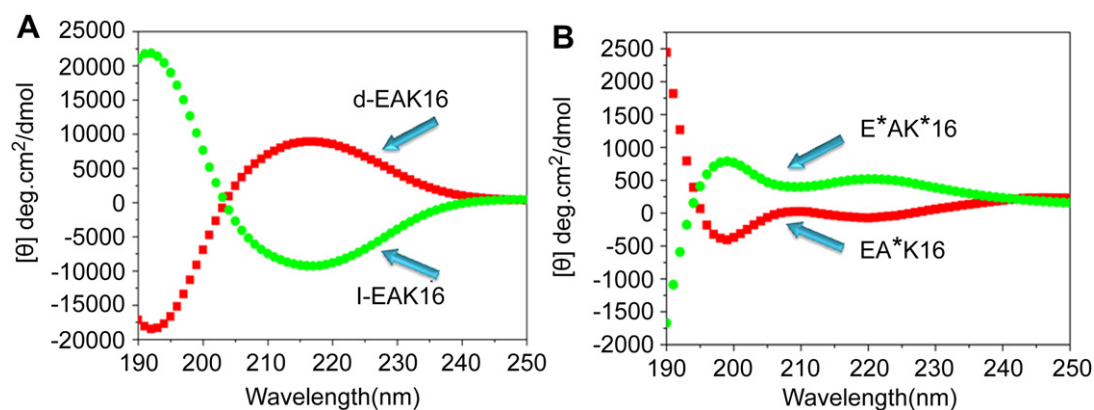

Fig. 2. Circular dichroism spectra of the peptides at 37 °C. A) Pair of d-EAK16 and l-EAK16, the l-EAK16 spectrum is the lower part and d-EAK16 spectrum is the upper part; B) Pair of EA*K16 and E*AK*16, EA*K16 spectrum is the lower part and E*AK*16 spectrum is the upper part. The 4 peptides showed stable secondary structures at the 37 °C. Note the completely inverted CD spectra for their chirality difference.
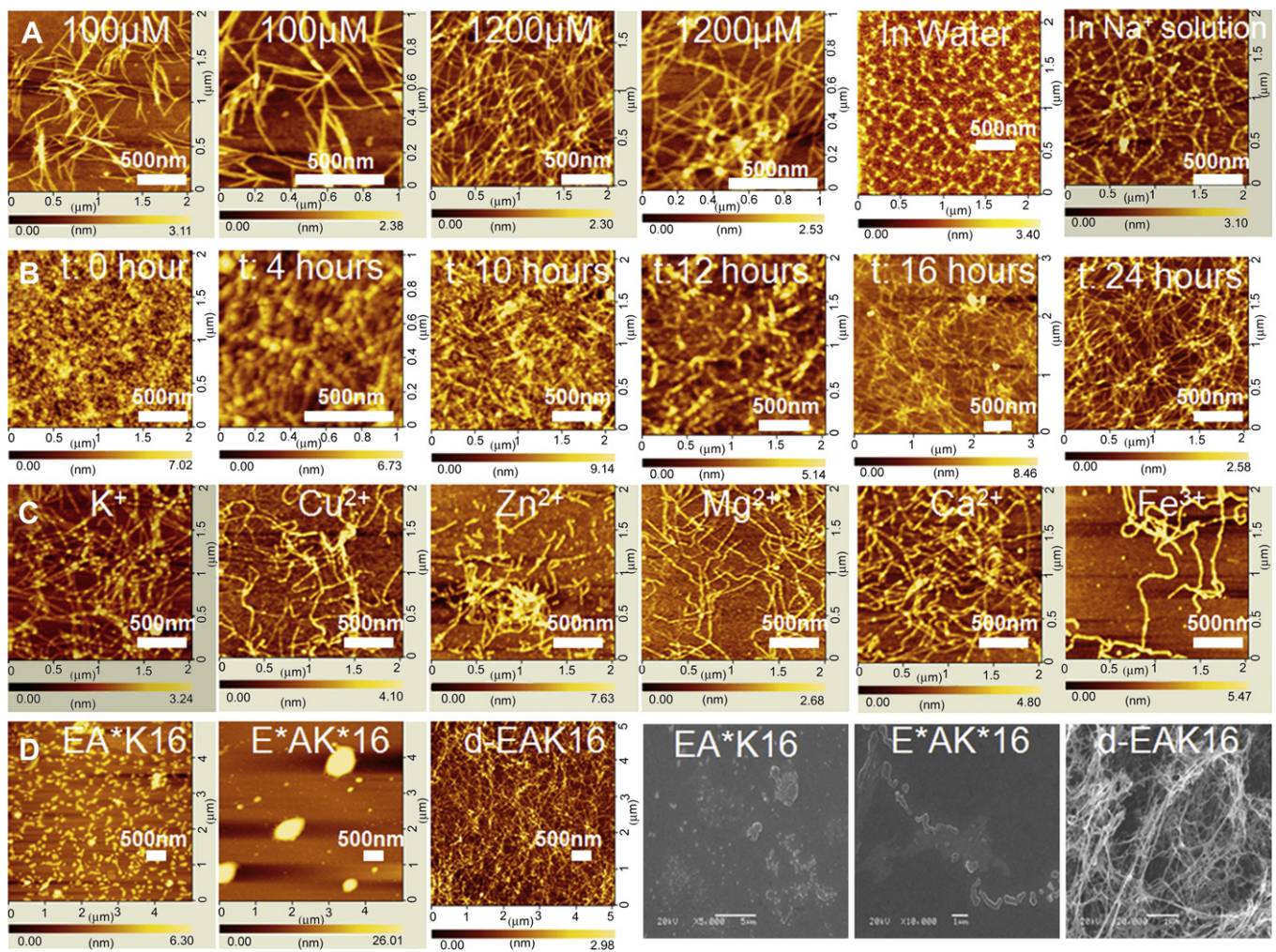
Fig. 3. AFM and SEM images of the self-assembling peptides. A) d-EAK16 self-assembled the ordered nanofibers at 100 μM or 1200 μM. The inter-spaces or pores of nanofibers are changed as a function of peptide concentrations; Peptide in water as a slow assembly control and peptide self-assembled in Na⁺ solution as a positive control). B) The time-dependent self-assembly process of d-EAK16 to nanofibers. AFM images showed these differences at 0, 4, 10, 12, 16 and 24 h. C) Various metal ions influence peptide self-assembly. d-EAK16 was incubated in various ionic solutions: K^+, Cu^{2+}, Zn^{2+}, Mg^{2+}, Ca^{2+}, Fe^{3+} (10 mM each). These metal ions influence the peptide self-assembly in different degrees. D) The AFM and SEM images to the chiral peptides at same condition: EA*K16, E*AK*16 and d-EAK16 (To better compare the structures of chiral peptides, here the SEM of d-EAK16 is zoomed in the SEM of reference [30] to 20000×). EA*K16 and E*AK*16 did not self-assemble to observable nanofibers under the same experimental conditions (results are not shown).

pure water reduces the speed of self-assembly [31]. We used AFM to follow d-EAK16 nanofiber formations from 0 to 24 h (Fig. 3B). At 0-h immediately after sonication, irregular particles were observed. At ~4 h, many short nanofibers appeared; 10 h later, most of them are self-assembling into ~200 nm nanofibers. At ~12 h, these short fibers lengthened and self-assembled further into longer nanofibers and some of them appeared to connect to each other. At ~16 h a majority of nanofibers form to 3D scaffold network. At ~24 h, d-EAK16 self-assembling into 3D nanofibers scaffold displayed a nanoscale structure like multi-layers of fishing-nets. It is clear that d-EAK16 undergoes dynamic self-assembly process to form well-ordered nanofiber scaffold in pure water, but salts significantly accelerate the process.

3.3.3. Various ion influences of d-EAK16 self-assembly

We asked what ions would influence the self-assembly, and placed d-EAK16 in 10 mM various ionic solutions including Na⁺, K^+, Cu^{2+}, Mg^{2+}, Zn^{2+}, Ca^{2+} and Fe^{3+} to mimic physiological ion concentration respectively. We used AFM to examine d-EAK16 nanofibers (Fig. 3C). The results might be associated with the hydrated radii contribution to self-assembly [1,32]. Comparing peptides in water, the ions play a key role in this process. Since we are interested in applying the scaffolds for physiological and clinical use to stop bleeding, it is relevant that blood contains these ions. As soon as d-EAK16 encounters blood, these ions can trigger the peptide immediately to undergo self-assembly into nanofibers.

3.3.4. Chirality influence for peptide self-assembly

We have previously reported that the peptides made using the same stereo-chemical amino acids, either all D- e.g. d-EAK16, or all L- e.g. l-EAK16, can self-assemble to ordered nanofibers. On the other hand, the peptides made of hetero-chiral amino acids such as the examples of EA*K16 and E*AK*16, their sequences contain alternating D- and L-amino acids. This alternating chiral configuration disrupts the usual uniform chiral backbone, thus they could not undergo self-assembly to form the nanofibers, but only form non-structured nano-aggregates (Fig. 3D). This result suggests homo-chirality is a key factor for peptide self-assembly. Furthermore, both CD spectra and AFM examinations suggest the sequences changed with hetero-chiral amino acids not only result in spectroscopic

changes but also inhibit the peptide self-assembly into nanofibers. Therefore, alternating hetero-chiral arrangements of D- and L-amino acid sequence are incompatible and unfavorable to useful nanofiber structural formation. Perhaps because the chiral heterogeneity not only interferes with the crucial non-covalent interactions, which in turn interferes with the formation of the supra-molecular nanofiber assembly.

3.4. Self-assembling nanofiber scaffolds for hemostasis

As we are interested in obtaining detailed information for hemostasis, we focused on the self-assembling peptides. These peptides can self-assemble themselves, which are different from chitosan and other biomaterials used in clinics and medical technology [33,34].

3.4.1. Agglutinating activity in vitro

We asked whether the self-assembling chiral peptides could have some medical and clinical benefits. We tested d-EAK16 and l-EAK16 in rabbit erythrocyte solution (Fig. 4A). Comparing to the negative control, there was a little agglutinating activity at 0.1 mg/ml and 0.5 mg/ml; when the concentration was increased to 1 mg/ml, the agglutinating activity become stronger; when the concentration was further increased to 2.5 mg/ml to 10 mg/ml, apparent agglutinating activity was observed (Fig. 4). However solutions of EA*K16 and E*A*K16 did not appear to have agglutinating activity. These observations are consistent that d-EAK16 and l-EAK16 which were capable to self-assemble into nanofibers but no nanofibers were observed for EA*K16 and E*A*K16 under the same conditions.

We also observed that the higher the peptide concentration, the more nanofibers, and the faster agglutinating activity became. Furthermore, we observed similar results for testing other erythrocytes including chicken, duck as well as 4 human blood types. We believe that ions and salts in the solution containing erythrocytes accelerated rapid peptide self-assembly into nanofibers.

3.4.2. Hemostasis in the vascularized rabbit liver wound healing model

We asked whether the self-assembling peptide d-EAK16 could stop bleeding in animals. In the transverse liver experiments, we made a sagittal liver cut in adult rabbit. Compared with the untreated controls (2 rabbits), the bleeding stop-time was ~80–120 s. When applied 200 μl of 1% (wt/vol) d-EAK16 solution to the wound (Fig. 4B), the hemostasis time is ~20 s (Fig. 4C). We also used 200 μl of 1% l-EAK16 that achieved hemostasis ~17 s (Fig. 4). In contrast, E*A*K16 and EA*K16 hemostasis times were ~70 and ~80 s, respectively (Fig. 4). Thus, our results suggest the alternating peptide chirality is less effective in hemostasis.

Comparing 2 pairs of chiral peptides, the pair of d-EAK16 and l-EAK16 not only formed nanofibers, but they also achieved rapid hemostasis. In contrast, the pair of EA*K16 and E*A*K16 did not form nanofibers, thus they could not stop bleeding rapidly. In a previous study, another self-assembling peptide RADA16 was shown to form nanofiber scaffolds and rapidly stop bleeding in rats but it is unsure what the underlying process may be [33]. Although there is little sequence and composition commonality between RADA16 and d-EAK16 or l-EAK16, they all achieved rapid hemostasis. Thus, they may share common structural features. However
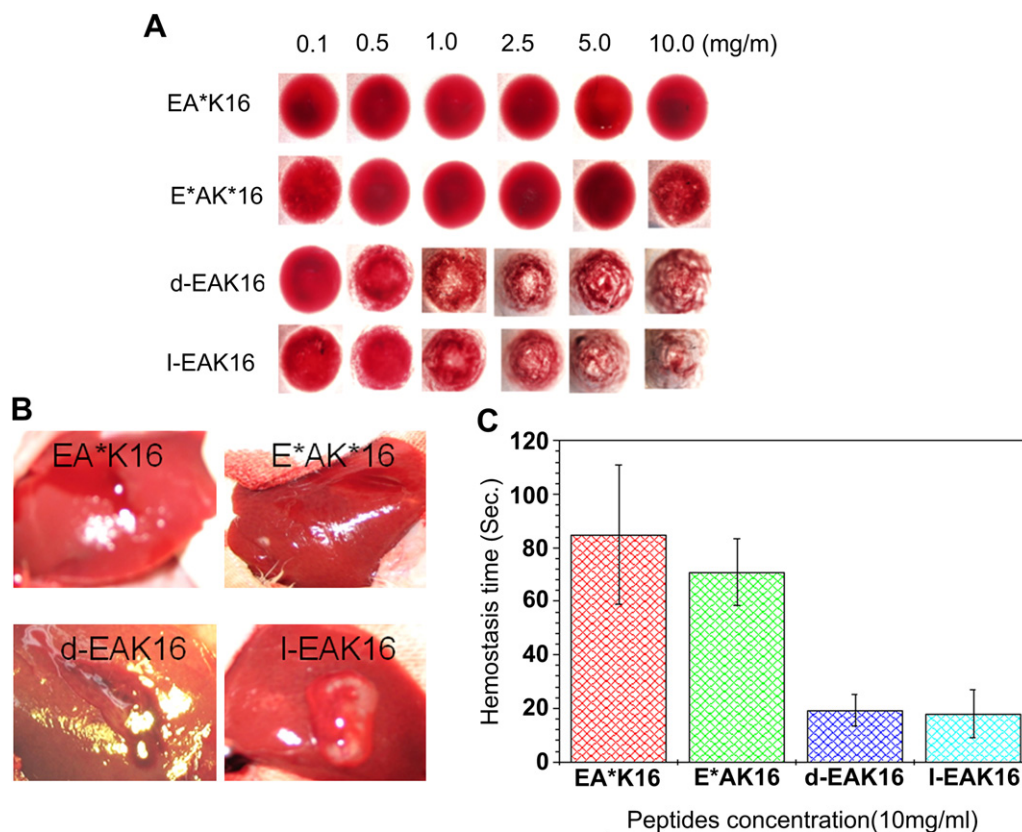

Fig. 4. Tests of erythrocyte aggregation activity *in vitro* and tests of rabbit liver hemostasis *in situ*. A) The optical microscopy images of rabbit erythrocyte aggregation *in vitro* for EA*K16, E*AK*16, d-EAK16 and l-EAK16. From left to right the peptide concentration is 0.1, 0.5, 1.0, 2.5, 5.0 and 10.0 mg/ml in each row. From up to down the peptides are EA*K16, E*AK*16, d-EAK16 and l-EAK16, respectively. B) The Rabbit liver hemostasis model *in situ*. d-EAK16 and l-EAK16 showed rapid hemostasis with ~20 s. However, when EA*K16 and E*AK*16 were applied to the liver cut, they could not stop the bleeding. C) EA*K16, E*AK*16, d-EAK16 and l-EAK16 hemostasis time. d-EAK16 and l-EAK16 showed rapid hemostasis, ~20 s, but E*AK*16 and EA*K16 are not as effective, took 70 and 80 s, respectively under the same experimental conditions.

the only common structural feature they all share is their ability to rapidly self-assemble into nanofiber scaffolds that correlate well with rapid hemostasis.

3.4.3. Rheological tests of chiral pairs of peptides

We are also interested in analyzing the gelation properties of chiral pairs of peptides, thus we carried out rheological studies from these 2 pairs of peptides. The rheological experiments measure 1) the storage modulus (G′), which measures material's elastic response (rigidity) to varying frequencies of applied oscillatory stress and 2) the loss modulus (G″), which measures material's viscous response and varying frequencies of applied oscillatory stress. Both d-EAK16 and l-EAK16 showed that the frequency G′ is greater than G″ (Fig. 5A,B). d-EAK16 and l-EAK16 and the storage modulus G′ reach to >1000 Pa. However, the storage modulus G′ of EA*K16 and E*AK*16 only reached ~4 Pa (Fig. 5C,D). The magnitude G′ of d-EAK16 and l-EAK16 is ~500 times higher than EA*K16 and ~1000 times higher than E*AK*16 (Fig. 5). Thus the mechanical properties of d-EAK16 and l-EAK16 are significantly different from EA*K16 and E*AK*16. The reasonable explanation is that the blood contains Na^+, K^+, Cu^{2+}, Mg^{2+}, Ca^{2+}, Zn^{2+} and Fe^{3+} that stimulate both homo-chiral peptides d-EAK16 and l-EAK16 to accelerate self-assembly into nanofibers that increase gelation therefore rapidly stop bleeding.

3.5. A plausible model for rapid hemostasis

From our current studies and previous reports [1], we summarized our results as following: 1) self-assembling peptides form nanofibers and these nanofibers form scaffolds, these scaffolds behave like a multiple layers of a "fishing-net" (Figs. 3 and 6C); 2) these peptides have a stable β-sheet secondary structure in physiological solution [29] and high temperature; 3) ions promote the peptide rapid self-assembly to form the nanofibers (Fig. 3); 4) d-EAK16 and l-EAK16 exhibit rapid hemostasis, but EA*K16 and E*AK*16 are less effective and this suggests that homo-chirality of peptide geometry is essential; 5) self-assembling peptides of d-EAK16 and l-EAK16 have similar rheological properties despite their chiral differences (Fig. 4).

Interestingly, it took ~16 h for d-EAK16 in pure water solution to self-assemble into nanofiber scaffold. However, d-EAK16 hemostasis time is ~20 s, we ask what is occurring during this process. A reasonable elucidation may be these various ions, proteins, enzymes and other factors in the blood cooperatively induce d-EAK16 self-assembly into nanofibers rapidly. In water, d-EAK16 does not self-assembly to nanofiber scaffold quickly, however, in salt and in blood, d-EAK16 rapidly self-assembled into nanofiber scaffolds.

In the normal hemostasis process, a high concentration of clotting factor at one location results in clotting, whereas the same number of molecules spread farther apart are less effective [35,36]. We showed that adding d-EAK16 and l-EAK16 solutions quickly stopped bleeding after d-EAK16 solution covered the wound surface (Fig. 4). It is perhaps that multiple ions and various proteins including coagulation factors in the blood absorbed to d-EAK16 and d-EAK16 assemblies. These Na^+, K^+, Cu^{2+}, Mg^{2+}, Ca^{2+}, Zn^{2+} and Fe^{3+} rapidly trigger the peptides to further self-assembly. With a stable secondary β-sheet molecular structure, the self-assembling
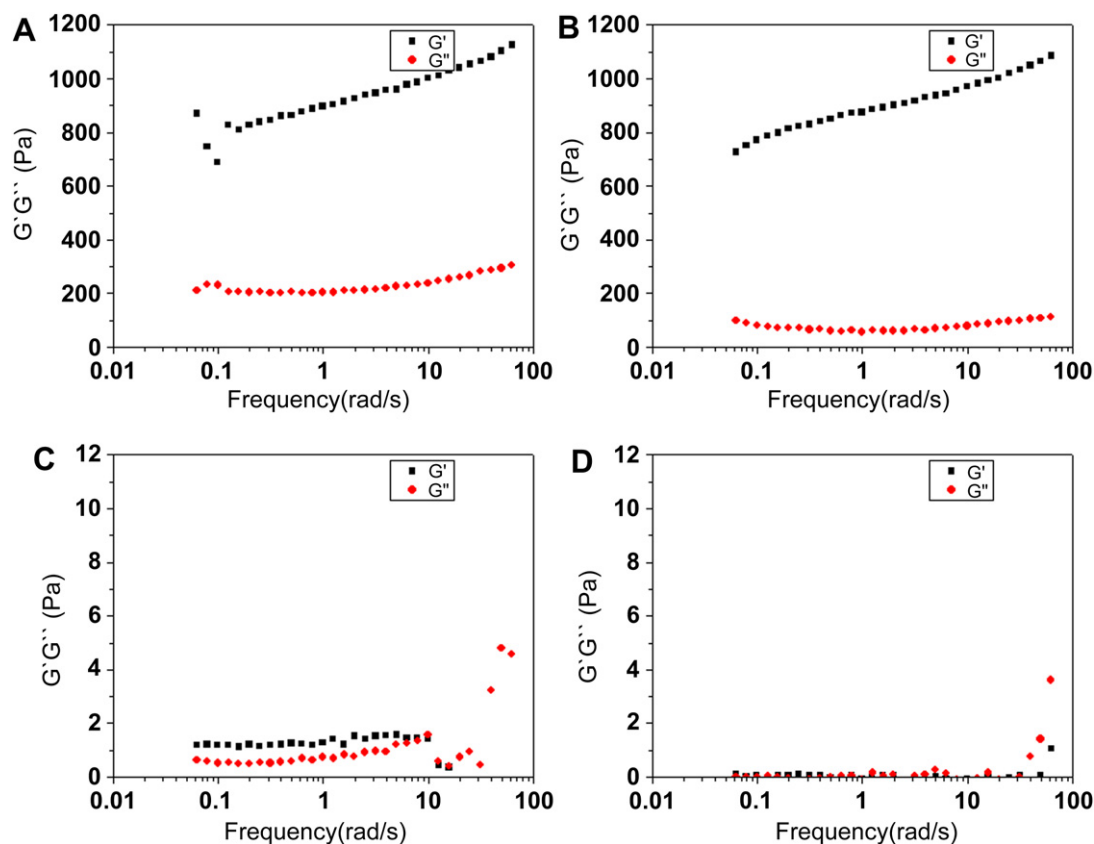

Fig. 5. Rheological tests for the chiral peptides. A) d-EAK16, B) l-EAK16, C) EA*K16, D) E*AK*16. The peptide solution to the rabbit blood was combined at 1:1 volume quickly and then ~500ul was transferred for rheological tests. The storage modulus G′ reached to >1000 Pa for both d-EAK16 and l-EAK16, but there were only 4 Pa for EA*K16 and E*AK*16. The rheology properties directly correlate with the peptide molecular structures, nanofiber scaffold formations, ability for gelation and their ability to stop bleeding rapidly.
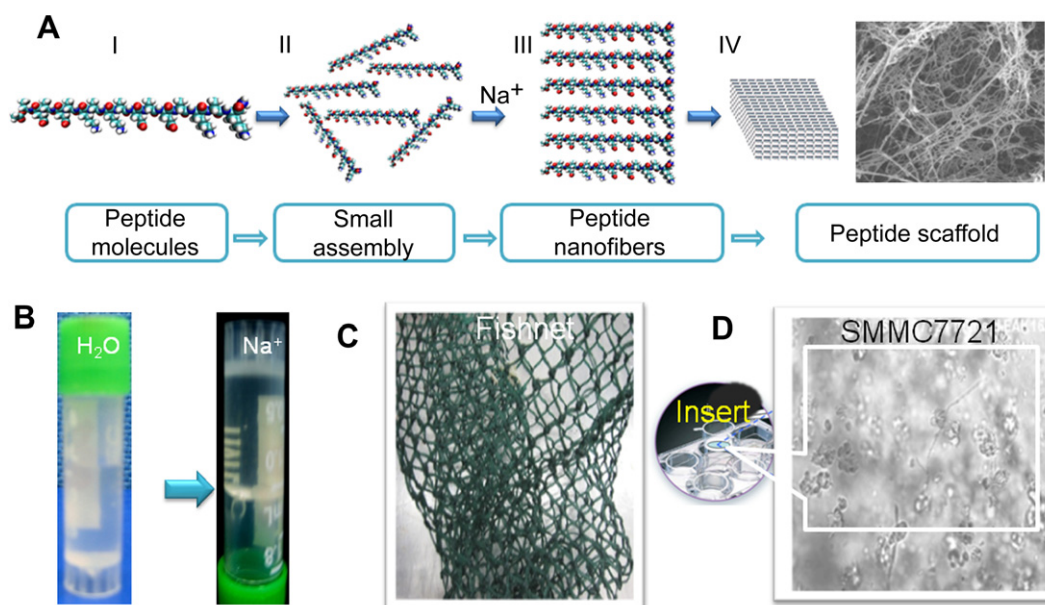
Fig. 6. Schematic illustration for a plausible model of self-assembling peptide d-EAK16 for rapid hemostasis. A) A molecular model of d-EAK16 peptide in a progressive self-assembly process. I) A single d-EAK16 peptide molecule, II) a few peptides in solution before self-assembly, III) self-assembling peptides form stable β-sheet structure and further form nanofibers, IV) self-assembling nanofiber scaffold (SEM). B) 1% d-EAK16 dissolved in the water (left, standing tube), and upon adding salt, d-EAK16 self-assemble to form transparent scaffold hydrogel (right, inverted tube). C) A photo of part of "fishing-net" is used as an analogy for the nanofiber scaffold, where multiple layers of the fish-net prevent escape of fish, even very small fish. Likewise, dense self-assembling peptide nanofiber scaffold resemble the multi-layered fish-net. Thus it prevents escape of the cells and fluid. D) d-EAK16 formed to transparent hydrogel that entrapped tissue cells in an insert tissue 3D cell culture system.

peptides already form short nanofibers, these short nanofibers immediately self-assemble into longer nanofiber scaffolds. Enzymes and other factors in the blood could enter into the nanofiber scaffold. Part of them could adsorb to the pores between the nanofibers. The nanofiber scaffold thus stop bleeding nano-mechanically by forming tight nano-seals to prevent leakage of liquid and cells.

3.6. Perspective of rapid hemostasis

There are three basic kinds of hemostatic phenomena: chemical, thermal, and mechanical [37], some limits and applicability of these hemostatic agents are known [35,36]. In surgery hemostasis requires a balance of bleeding, clotting and timing to stop it. In the self-assembling peptide system, we exploit a nano-mechanical phenomenon where numerous nanofibers form scaffolds and resemble multiple layered fishing-nets. These nano-fishing-nets prevent the blood cells and other molecules escape from the cut or wound sites. This idea is supported by the fact that although d-EAK16, l-EAK16 and a previous studied l-RADA16 [33] have different composition and chirality, they share a common stable β-sheet molecular structure, and they self-assemble from the soluble peptide molecules into insoluble nanofibers scaffolds that is a hydrogel of 99% water. These nanofiber scaffold hydrogels effectively stop bleeding in a few to tens of seconds. Our study shows that the new designer self-assembling peptide d-EAK16 nanofiber scaffold may have many clinical applications not only for surgery to stop bleeding quickly, but also for chronic wound care.

4. Conclusion

Our studies here not only provide insight into the importance of homo-chirality for both the structure and nanofiber scaffold hydrogel properties of peptides, but also for the application of nanofiber scaffold relationship to rapid hemostasis. It is possible that our research will likely further stimulate others to design new

biological materials at single amino acid level. Since D-form peptides resist protease degradation, our research using chiral D-form self-assembling peptides may further broaden applications of fabrication self-assembling D-peptides in clinical and medical nanobiotechnology.

Contributors

Z.L. and S.Z. designed research; Z.L. and S.Z. contributed new reagents and analytic tools; Z.L., S.W. and S.Z. analyzed data; Z.L. and S.Z. wrote the paper.

Conflict of interest statement
The authors declare no conflict of interest.

Appendix

Figures with essential color discrimination. Figs. 1–6 in this article have parts that are difficult to interpret in black and white. The full color images can be found in the online version, at doi: 10.1016/j.biomaterials.2010.11.049

References

[1] Zhang S, Holmes T, Lockshin C, Rich A. Spontaneous assembly of a self-complementary oligopeptide to form a stable macroscopic membrane. Proc Natl Acad Sci U S A 1993;90:3334–8.

[2] Yeh JI, Shoucheng D, Tortajada A, Paulo J, Zhang S. Peptergents: peptide detergents that improve stability and functionality of a membrane protein, glycerol- 3-phosphate dehydrogenase. Biochemistry 2005;44:16912–9.

[3] Zhao X, Nagai Y, Reeves PJ, Kiley P, Khorana HG, Zhang S. Designer lipid-like peptides significantly stabilize G-protein coupled receptor bovine rhodopsin. Proc Natl Acad Sci U S A 2006;103:17707–12.

[4] Matsumoto K, Vaughn M, Bruce BD, Koutsopoulos S, Zhang S. Designer peptide surfactants stabilize functional photosystem-I membrane complex in aqueous solution for extended time. J Phys Chem B 2009; 113:75–83.

[5] Keyes-Baig C, Duhamel J, Fung S-Y, Bezaire J, Chen P. Self-assembling peptide as a potential carrier of hydrophobic compounds. J Am Chem Soc 2004;126: 7522–32.

[6] Nagai Y, Unsworth LD, Koutsopoulos S, Zhang S. Slow release of molecules in self-assembling peptide nanofiber scaffold. J Control Release 2006;115: 18–25.

[7] Gelaina F, Unsworthb LD, Zhang S. Slow and sustained release of active cytokines from self-assembling peptide scaffolds. J Control Release 2010;145: 231–9.

[8] Koutsopolous S, Unsworth L, Nagai Y, Zhang S. Slow release of functional proteins through designer self-assembling peptide nanofiber hydrogel scaffolds. Proc Natl Acad Sci U S A 2009;106:4623–8.

[9] Das R, Kiley PJ, Sega M, Norville J, Yu AA, Wang L, et al. Integration of photosynthetic protein molecular complexes in solid-state electronic devices. Nano Lett 2004;4:1079–83.

[10] Kiley P, Zhao X, Vaughn M, Baldo MA, Bruce BD, Zhang S. Self-assembling peptide detergents stabilize isolated photosystem I on a dry surface for an extended time. PLoS Biol 2005;3:1180–6.

[11] Zhang S, Holmes T, DiPersio M, Hynes RO, Su X, Rich A. Self-complementary oligopeptide matrices support mammalian cell attachment. Biomaterials 1995;16:1385–93.

[12] Gelain F, Lomander A, Vescovi AL, Zhang S. Designer self-assembling peptide nanofiber scaffolds for adult mouse neural stem cell 3-dimensional cultures. PLoS ONE 2006;1:e119.

[13] Horii A, Wang X, Gelain F, Zhang S. Biological designer self-assembling peptide nanofiber scaffolds significantly enhance osteoblast proliferation, differentiation and 3-D migration. PLoS ONE 2007;2:e190.

[14] Wang X, Horii A, Zhang S. Designer functionalized self-assembling peptide nanofiber scaffolds for growth, migration, and tubulogenesis of human umbilical vein endothelial cells. Soft Matter 2008;4:2388–95.

[15] Kumada Y, Zhang S. Significant type I and type III collagen production from human periodontal ligament fibroblasts in 3D peptide scaffolds without extra growth factors. PLoS ONE 2010;5:e10305.

[16] Kisiday J, Jin M, Kurz B, Hung H, Semino C, Zhang S, et al. Self-assembling peptide hydrogel fosters chondrocyte extracellular matrix production and cell division: implications for cartilage tissue repair. Proc Natl Acad Sci U S A 2002;99:9996–10001.

[17] Davis ME, Motion JPM, Narmoneva DA, Takahashi T, Hakuno D, Kamm RD, et al. Injectable self-assembling peptide nanofibers create intramyocardial microenvironments for endothelial cells. Circulation 2005;111:442–50.

[18] Davis ME, Hsieh PCH, Takahashi T, Song Q, Zhang S, Kamm RD, et al. Local myocardial insulin-like growth factor 1 (IGF-1) delivery with biotinylated peptide nanofibers improves cell therapy for myocardial infarction. Proc Natl Acad Sci U S A 2006;103:8155–60.

[19] Guo J, Su H, Zeng Y, Liang Y-X, Wong WM, Ellis-Behnke RG, et al. Reknitting the injured spinal cord by self-assembling peptide nanofiber scaffold. Nano-medicine 2007;3:311–21.

[20] Guo J, Leung KKG, Su H, Yuan Q, Wang L, Chu T-H, et al. Self-assembling peptide nanofiber scaffold promotes the reconstruction of acutely injured brain. Nanomedicine 2009;5:345–51.

[21] Zhang S. Emerging biological materials through molecular self-assembly. Biotechnol Adv 2002;20:321–39.

[22] Schneider JP, Pochan DJ, Ozbas B, Rajagopal K, Pakstis L, Kretsinger J. Responsive hydrogels from the intramolecular folding and self-assembly of a designed peptide. J Am Chem Soc 2002;124:15030–7.

[23] Niece KL, Hartgerink JD, Donners JJJM, Stupp SI. Self-assembly combining two bioactive peptide-amphiphile molecules into nanofibers by electrostatic attraction. J Am Chem Soc 2003;125:7146–7.

[24] Ryadnov MG, Woolfson DN. Engineering the morphology of a self-assembling protein fibre. Nat Mater 2003;2:329–32.

[25] Zhang S. Fabrication of novel biomaterials through molecular self-assembly. Nat Biotechnol 2003;21:1171–8.

[26] Percec V, Dulcey AE, Balagurusamy VSK, Miura Y, Smidrkal J, Peterca M, et al. Self-assembly of amphiphilic dendritic dipeptides into helical pores. Nature 2004;430:764–8.

[27] Ashkenasy N, Horne WS, Ghadiri MR. Design of self-assembling peptide nanotubes with delocalized electronic states. Small 2005;2:99–102.

[28] Zhang S. Designer self-assembling peptide nanofiber scaffolds for study of 3-D cell biology and beyond. Adv Cancer Res 2008;99:335–62.

[29] Luo Z, Zhao X, Zhang S. Structural dynamic of a self-assembling peptide d-EAK16 made of only D-amino acids. PLoS ONE 2008;3:e2364.

[30] Luo Z, Zhao X, Zhang S. Self-organization of a chiral D-EAK16 designer peptide into a 3D nanofiber scaffold. Macromol Biosci 2008;8:785–91.

[31] Yokoi H, Kinoshita T, Zhang S. Dynamic reassembly of peptide RADA16 nanofiber scaffold. Proc Natl Acad Sci U S A 2005;102:8414–9.

[32] Pauling L. Nature of the chemical bond and the structure of molecules and crystals:an introduction to model structrual chemistry. 3rd ed. Ithaca, NY: Cornel Univ. Press; 1960.

[33] Ellis-Behnke RG, Liang Y-X, Tay DKC, Kau PWF, Schneider GE, Zhang S, et al. Nano hemostat solution: immediate hemostasis at the nanoscale. Nano-medicine 2006;2:207–15.

[34] Ellis-Behnke RG, Liang Y-X, You S-W, Tay DKC, Zhang S, So K-F, et al. Nano neuro knitting: peptide nanofiber scaffold for brain repair and axon regeneration with functional return of vision. Proc Natl Acad Sci U S A 2006;103:5054–9.

[35] Deloughery TG. In: Hemostasis and thrombosis. 2nd ed. Georgetown, Texas U.S.A: Landes Bioscience; 2004.

[36] Andrew Blann D, Lip GY, Turpie AG. Thrombosis in clinical practice. London, U.K: Taylor & Francis; 2005.

[37] Davie EW, Ratnoff OD. Waterfall sequence of intrinsic blood coagulation. Science 1964;145:1310–2.